Steady Three-Dimensional Flow of a Walter's B' Fluid in a Vertical Channel

Serdar BARIŞ
University of İstanbul, Faculty of Engineering,
Department of Mechanical Engineering,
İstanbul-TURKEY

Abstract

Steady three-dimensional flow of a Walter's B' fluid in a vertical channel was investigated. It is assumed that the fluid is injected into the channel through one side of the channel. The combined effects of viscoelasticity and inertia are considered. By using the appropriate similarity transformations for the velocity components and temperature, the basic equations governing flow and heat transfer are reduced to a set of ordinary differential equations. These equations were solved approximately subject to the relevant boundary conditions with a numerical technique. The effect of the elasticity of the fluid on the flow and heat transfer on the walls of the channel are discussed.

Key words: Walter's B' fluid, Vertical channel, Viscoelasticity, Injection.

Introduction

The flow of Newtonian and non-Newtonian fluids in a porous surface channel has always attracted the interest of many investigators in view of its applications in engineering practice. Examples of these are the cases of boundary layer control, transpiration cooling, and gaseous diffusion. In boundary layer control, the decelerated fluid particles in the boundary layer are removed through slits in the wall into the interior of the body. With sufficiently strong suction, separation can be prevented. An alternative method of preventing separation consists in supplying additional energy to the particles of fluid which are being retarded in the boundary layer. This result can be achieved by discharging fluid from the interior of the body with the aid of a special blower (Schlichting, 1968). In transpiration cooling, the walls of a channel carrying a hot fluid are made of a porous material through which fluid is injected to form a protective layer of cooler fluid near the wall. In separating U_{235} from U_{238} by gaseous diffusion, the uranium is first converted to the gas UF_6. The gas is then forced through a porous wall by a pressure gradient. The difference in the molecular weights causes differences in the rates of diffusion through the porous material. This results in a concentration of the desired component (Skalak and Wang, 1978). In addition to applications mentioned above, blowing is used to add reactants, prevent corrosion and reduce drag. Suction is applied to chemical processes to remove reactants.

In view of its importance, the flow of Newtonian and non-Newtonian fluids through porous channels has been investigated by numerous authors. The case of a two-dimensional, incompressible, steady, laminar suction flow of a Newtonian fluid in a parallel-walled porous channel was studied by Berman (1953). He solved the Navier-Stokes equations by using a perturbation method for very low cross-flow Reynolds numbers. After his pioneering work, this problem has been studied by many researchers considering various variations in the problem, see, e.g., Cox (1991) and Choi *et al.* (1999) and references cited in these articles.

Wang and Skalak (1974) were the first to present

the solution for a three-dimensional problem of fluid injection through one side of a long vertical channel for Newtonian fluid. They obtained a series solution valid for small values of the cross-flow Reynolds number and a numerical solution for both small and large cross-flow Reynolds numbers. Huang (1978) re-examined Wang and Skalak's problem using a method based upon quasilinearization. The same flow problem was solved for large cross-flow Reynolds numbers by Ascher (1980) using a spline-collocation method. Sharma and Chaudhary (1982) reconsidered the above-mentioned problem by introducing a second order viscoelastic fluid. They obtained the second order perturbation solution by assuming that the cross-flow Reynolds number is small. However, their results seem to be in error; their expression for pressure does not satisfy the equations of motion. In a recent paper, Barış (2001) investigated Wang and Skalak's problem by replacing Newtonian fluid by thermodynamically compatible fluid of second grade. In his study, perturbation solutions of the velocity field have been obtained by taking the elastic number as the perturbation parameter. From a technological point of view, flows of this type are always important, especially in transpiration cooling, which is a very effective process to protect certain structural elements in turbojet and rocket engines, like combustion chamber walls, or gas turbine blades, from the influence of hot gases (Singh, 1999).

A literature survey clearly indicates that little attention has been paid to the three-dimensional flows of non-Newtonian fluids in a vertical channel. In view of the increasing importance of viscoelastic fluids in engineering practice, such a problem involving the steady three-dimensional flow of an idealized elastico-viscous fluid (more specifically such a fluid is called a Walter's B′ fluid) in a vertical channel is investigated here. Our main purpose is to examine qualitatively the effect of elasticity of the fluid on the flow and heat transfer on the walls of the channel for the problem under discussion.

Formulation of the Problem

There are numerous models of viscoelastic fluids suggested in the literature. To get some insight into their flow behaviour, it is preferable to restrict to a model with a minimum number of parameters in the constitutive equations. We have chosen the model of Walter's B′ fluid for our study as it involves only one non-Newtonian parameter. The Cauchy stress

tensor $\mathbf{T}$ in such a fluid is related to the motion in the following manner (Beard and Walters, 1964):

$$\mathbf{T} = -p\mathbf{I} + 2\eta_0\mathbf{e} - 2k_0\frac{\delta\mathbf{e}}{\delta t} \qquad (1)$$

In this equation, p is the pressure, $\mathbf{I}$ is the identity tensor, and the rate of strain tensor $\mathbf{e}$ is defined by

$$2\mathbf{e} = \nabla\mathbf{v} + (\nabla\mathbf{v})^T \qquad (2)$$

where $\mathbf{v}$ is the velocity vector, ∇ is the gradient operator, and $\delta/\delta t$ denotes the convected differentiation of a tensor quantity in relation to the material in motion. The convected differentation of the rate of strain tensor is given by

$$\frac{\delta\mathbf{e}}{\delta t} = \frac{\partial\mathbf{e}}{\partial t} + \mathbf{v}\cdot\nabla\mathbf{e} - \mathbf{e}\cdot\nabla\mathbf{v} - (\nabla\mathbf{v})^T\cdot\mathbf{e} \qquad (3)$$

Finally η_0 and k_0 are, respectively, the limiting viscosity at small rate of shear and the short memory coefficient which are defined through

$$\eta_0 = \int_0^\infty N(\tau)d\tau, \qquad k_0 = \int_0^\infty \tau N(\tau)d\tau \qquad (4)$$

where $N(\tau)$ is the distribution function with relaxation time τ. This idealized model is a valid approximation of Walter's B′ fluid taking very short memory into account so that terms involving

$$\int_0^\infty \tau^n N(\tau)d\tau, n \geqslant 2 \qquad (5)$$

have been neglected. For a detailed description of this model the reader should consult Beard and Walters (1964).

Figure 1 shows the physical model and coordinate system. A fluid is injected through a vertical porous plate at y = d with uniform velocity U. The fluid strikes another vertical impermeable plate at y = 0. It flows out through the opening of the plates, due to the action of gravity along the z-axis. We have further assumed the distance between the walls, d, is small compared to the dimensions of the plates, i.e. L >> B >> d. Due to this assumption the edge effects can be ignored and the isobars are parallel to the z-axis.
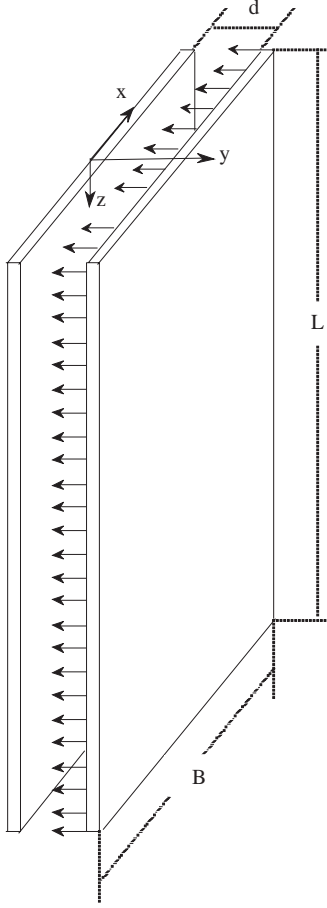
Figure 1. Sketch of flow geometry and coordinate system

In addition to Eq. (1), the basic equations of the problem are the following:
Continuity equation:

$$\nabla \cdot \mathbf{v} = 0, \qquad (6)$$

Equations of motion:

$$\rho(\mathbf{v} \cdot \nabla \mathbf{v}) = \nabla \cdot \mathbf{T} + \rho \mathbf{g}, \qquad (7)$$

Energy equation:

$$\rho c_p(\mathbf{v} \cdot \nabla T) = k\Delta T, \qquad (8)$$

where ρ is the density, $\mathbf{g}$ the gravitational acceleration vector, T the temperature, c_p the specific heat at constant pressure, k the thermal conductivity and Δ the Laplacian operator. The assumptions made in the above equations are as follows: (a) The flow is steady and laminar; (b) The fluid is incompressible; (c) The body force per unit mass is taken to be equal to the gravitational acceleration; (d) All the physical properties, e.g. viscosity, specific heat and thermal conductivity of the fluid, remain invariable throughout the fluid; (e) The heat flux vector can be represented by Fourier's law; (f) The effects of radiant heating and viscous dissipation are negligible.

Substituting Cauchy stress tensor from Eq. (1) into equations of motion (7), with the aid of Eqs. (2) and (3), we get

$$
\begin{aligned}
\rho(\mathbf{v} \cdot \nabla \mathbf{v}) = \quad & -\nabla p + \rho \mathbf{g} + \eta_0 \nabla^2 \mathbf{v} \\
& -2k_0 \mathbf{v} \cdot \nabla \nabla^2 \mathbf{v} + k_0 \nabla^2(\mathbf{v} \cdot \nabla \mathbf{v})
\end{aligned}
\qquad (9)
$$

The velocity components corresponding to the x, y and z directions are respectively denoted by u, v and w. Following Wang and Skalak (1974), we look for a solution, compatible with the continuity equation (6), of the form

$$u = \frac{U}{d} x f'(\eta), v = -U f(\eta), w = \frac{d^2 g \rho}{\eta_0} h(\eta), \quad (10)$$

where $\eta = y/d$ and the prime denotes the differentiation with respect to η.
The boundary conditions for the velocity field are

$$
\begin{aligned}
\eta = 0 &: f(0) = 0, f'(0) = 0, h(0) = 0, \\
\eta = 1 &: f(1) = 1, f'(1) = 0, h(1) = 0.
\end{aligned}
\qquad (11)
$$

It follows from Eq.(10) and the equation of motion (9) that

$$
\begin{aligned}
\frac{\partial p}{\partial x} = \quad & \frac{Ux}{d^2}\left(-U\rho f'^2 + U\rho f f'' + \frac{Uk_0}{d^2}f''^2 + \frac{\eta_0}{d}f''' \right. \\
& \left. -\frac{2Uk_0}{d^2}f'f''' + \frac{Uk_0}{d^2}ff^{IV}\right),
\end{aligned}
\qquad (12)
$$

$$\frac{\partial p}{\partial \eta} = -U^2 \rho f f' - \frac{U\eta_0}{d}f'' + \frac{3U^2 k_0}{d^2}f'f'' - \frac{U^2 k_0}{d^2}ff''', \qquad (13)$$

$$h'' + Refh' + ReS(fh''' - f''h' - 2f'h'') + 1 = 0, \qquad (14)$$

where the cross-flow Reynolds number, Re, and the elastic number, S, are defined through, respectively

$$Re = \frac{Ud\rho}{\eta_0}, S = \frac{k_0}{\rho d^2}. \quad (15)$$

Integrating Eq. (13) with respect to η, we get

$$p(x,\eta) = \quad -\frac{1}{2}\rho U^2 f^2 - \frac{U\eta_0}{d}f' + \frac{2U^2 k_0}{d^2}f'^2$$
$$-\frac{U^2 k_0}{d^2}ff'' + \phi(x), \quad (16)$$

where $\phi(x)$ is an arbitrary function of x. Differentiation of the above equation with respect to x yields

$$\frac{\partial p}{\partial x} = \frac{d\phi}{dx}. \quad (17)$$

Combining Eqs. (12) and (17), we obtain

$$\frac{d\phi}{dx} = \quad \frac{Ux\eta_0}{d^3}\left\{f''' + Re(ff'' - f'^2)\right.$$
$$\left. + ReS(ff^{IV} + f''^2 - 2f'f''')\right\}. \quad (18)$$

It is apparent that the quantity in parentheses in Eq. (18) must be independent of η. Hence, we have the following equation for f:

$$f''' + Re(ff'' - f'^2) + ReS(ff^{IV} + f''^2 - 2f'f''') = C, \quad (19)$$

where C is an arbitrary constant which takes the value

$$C = f'''(0) + ReSf''^2(0). \quad (20)$$

Now we differentiate Eq. (19) with respect to η to eliminate the constant C. This gives

$$f^{IV} + Re(ff''' - f'f'') + ReS(ff^V - f'f^{IV}) = 0. \quad (21)$$

By using Eq. (19), $\phi(x)$ can now be written as

$$\phi(x) = \frac{U\eta_0 C}{2d^3}x^2 + p_0, \quad (22)$$

where p_0 is the constant of integration.

Inserting $\phi(x)$ from Eq. (22) into Eq. (16), we have

$$p(x,\eta) = \quad -\frac{1}{2}\rho U^2 f^2 - \frac{U\eta_0}{d}f' + \frac{2U^2 k_0}{d^2}f'^2$$
$$-\frac{U^2 k_0}{d^2}ff'' + \frac{U\eta_0 C}{2d^3}x^2 + p_0. \quad (23)$$

If one can solve Eq. (21) under the related boundary conditions, Eq. (23) gives the pressure at any point.

From Eq. (23), the pressure variations in the x and y directions can be written in non-dimensional form as follows:

$$P_x = \frac{p(0,\eta) - p(x,\eta)}{\rho U^2} = -\frac{\{f'''(0) + ReSf''^2(0)\}}{2Re}\left(\frac{x}{d}\right)^2, \quad (24)$$

$$P_y = \frac{p(x,0) - p(x,\eta)}{\rho U^2} = \frac{f^2}{2} + \frac{f'}{Re} + S(ff'' - 2f'^2) \quad (25)$$

It is also interesting to determine the effect of the elastic parameter S on the shear stresses on the walls of the channel. From Eqs. (1)-(3) and (10), we obtain

$$\tau_{xy}(0) = \frac{T_{xy}(0)d^2}{\eta_0 Ux} = f''(0), \tau_{xy}(1) = \frac{T_{xy}(1)d^2}{\eta_0 Ux}$$
$$= f''(1) + ReSf'''(1), \quad (26)$$

$$\tau_{zy}(0) = \frac{T_{zy}(0)}{\rho gd} = h'(0), \tau_{zy}(1) = \frac{T_{zy}(1)}{\rho gd}$$
$$= h'(1) + ReSh''(1) \quad (27)$$

The terms in Eqs. (14) and (21) having Re S factor represent the non-Newtonian character of the fluid. It is noticed that the presence of elasticity in the fluid yields third- and fifth-order differential equations, whereas in the Newtonian case (S = 0) the orders of Eqs. (14) and (21) are two and four, respectively. It would thus appear that the additional boundary conditions must be imposed to obtain a solution. In order to overcome this difficulty, we seek a solution of Eqs. (14) and (21) of the form

$$f = f_0 + Sf_1 + O(S^2), \qquad (28)$$

$$h = h_0 + Sh_1 + O(S^2), \qquad (29)$$

valid for sufficiently small S. Inserting Eqs. (28) and (29) into Eqs. (14) and (21), and equating the corresponding coefficient of S up to first order, the following set of ordinary differential equations is obtained

$$f_0^{IV} + Re(f_0 f_0''' - f_0' f_0'') = 0, \qquad (30)$$

$$f_1^{IV} + (Re f_0)f_1''' - (Re f_0')f_1'' - (Re f_0'')f_1' \\ + (Re f_0''')f_1 = Re(f_0' f_0^{IV} - f_0 f_0^V), \qquad (31)$$

$$h_0'' + (Re f_0)h_0' = -1, \qquad (32)$$

$$h_1'' + (Re f_0)h_1' = Re(f_0'' h_0 + 2f_0' h_0'' - f_0 h_0''' - f_1 h_0'), \qquad (33)$$

In a similar manner, the higher order terms can be obtained, but the calculations will become complicated. Moreover, the solutions considered are valid for small values of S. Therefore, we retain up to first order terms. From Eqs. (11), (28) and (29) it follows that the boundary conditions for Eqs. (30)-(33) are

$$f_0(0) = 0, f_0'(0) = 0, f_0(1) = 1, f_0'(1) = 0, \qquad (34)$$

$$f_1(0) = 0, f_1'(0) = 0, f_1(1) = 0, f_1'(1) = 0, \qquad (35)$$

$$h_0(0) = 0, h_0(1) = 0, \qquad (36)$$

$$h_1(0) = 0, h_1(1) = 0, \qquad (37)$$

It is recorded that for Newtonian fluid (S = 0) Eqs. (30) and (32) together with the associated boundary conditions (34) and (36) are the same as

those obtained by Wang and Skalak (1974). In addition, Eq. (30) with different boundary conditions represents the two-dimensional flow of a Newtonian fluid in a channel with porous walls (White *et al.*, 1958; Terrill and Shrestha, 1965).

The integration of Eqs. (30)-(33) subject to the related boundary conditions (34)-(37) has been performed numerically.

Next, we introduce a temperature field of the form

$$T = T_0 + (T_1 - T_0)\theta(\eta), \qquad (38)$$

where T_0 and T_1 are temperatures (constant in value) of the impermeable and porous plates, respectively. Substituting Eqs. (10) and (38) into Eq. (8) leads to the ordinary differential equation

$$\theta'' + Pef\theta' = 0, \qquad (39)$$

where $Pe = \rho U d c_p / k$ is the Peclet number. Equation (39) is to be solved subject to the boundary conditions

$$\theta(0) = 0, \theta(1) = 1. \qquad (40)$$

In order to solve Eq. (39), f_0 and f_1 functions are first determined from Eqs. (30) and (31) and it can be then solved numerically.

Numerical Results and Discussion

Several numerical methods can be used to solve the above differential equations. One convenient and accurate method, which we will use here, is the so-called shooting method. Firstly, these equations, together with the associated boundary conditions, are reduced to first-order differential equations. Later, for given values of the parameters, the unknown initial conditions at the initial point ($\eta = 0$) are roughly estimated and the differential equation is processed by using the fourth-order Runge-Kutta procedure from $\eta = 0$ to $\eta = 1$, as though we had an initial value problem. The mathematical problem is to find the correct values of the unknown initial conditions which yield the known values of the functions under consideration at the terminal point ($\eta = 1$). Since for Re = 0 the analytical solution provides exact initial values for these functions, successive numerical solutions can be generated as Re is increased. The accuracy of the assumed missing initial conditions are checked by comparing the calculated values of

the above-mentioned functions at the terminal point with their given values there. If a difference exists, the computations with new and improved initial values are repeated. This process is continued until the agreement between the calculated and known values at the terminal point is within the specified degree of accuracy. The systematic way used here for finding values of the missing initial conditions is equivalent to a modified Newton's method for finding the roots of equations in several variables. The accuracy of missing initial conditions which yield the known values at the terminal point is at least 10^{-6}. The results are summarized in Table 1.

Since our perturbation analysis is valid only for small values of elastic number S, the variation of S is limited to the range from 0.0 to 0.025. In addition, the numerical solutions obtained for the problem under consideration point to the conclusion that the perturbation solutions, even though obtained without making any assumption on the size of the cross-flow Reynolds number Re, give acceptable results only when $Re \leqslant 20$. For S > 0.025 and Re > 20, since the effects of successive terms in the perturbation expansion are more significant, i.e. $|Sf_1| > |f_0|$ and $|Sh_1| > |h_0|$, the perturbation solutions fail to give satisfactory results, that is, the solutions cannot be trusted to be meaningful.
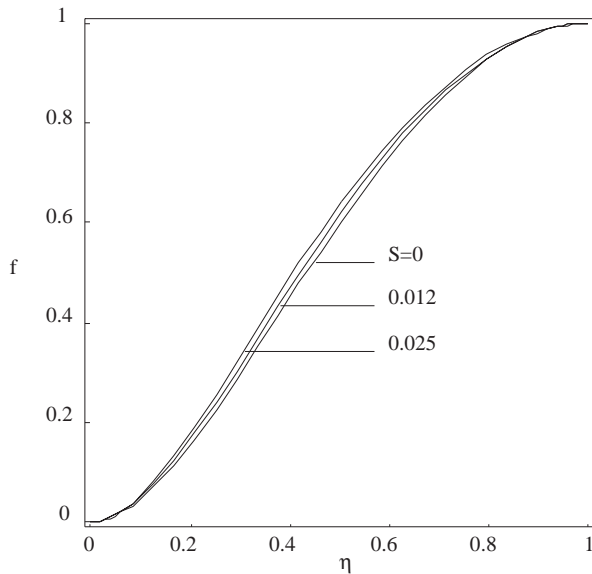
Figure 2. Normal velocity profiles for Re = 10

In Figures 2 to 7, the functions which correspond to the velocity components are plotted versus η for two different values of the cross-flow Reynolds number Re, with the elastic number S as a parameter. For low values of the cross-flow Reynolds number,

e.g. Re = 1, the velocity profiles in the viscoelastic fluid case, are indistinguishable from those in the Newtonian fluid case and so they are not presented.
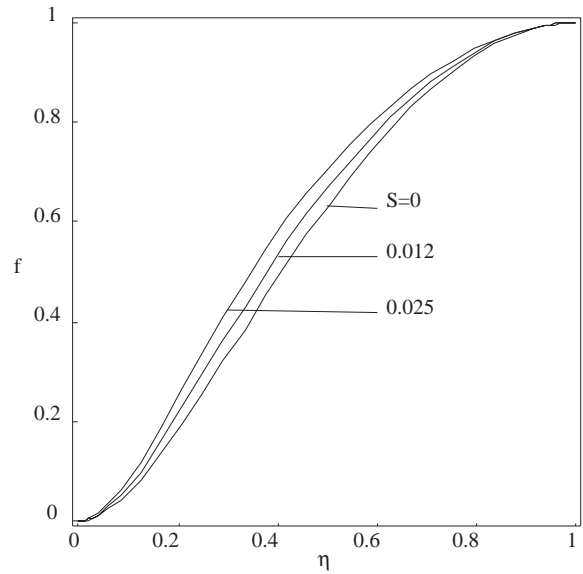
Figure 3. Normal velocity profiles for Re = 20
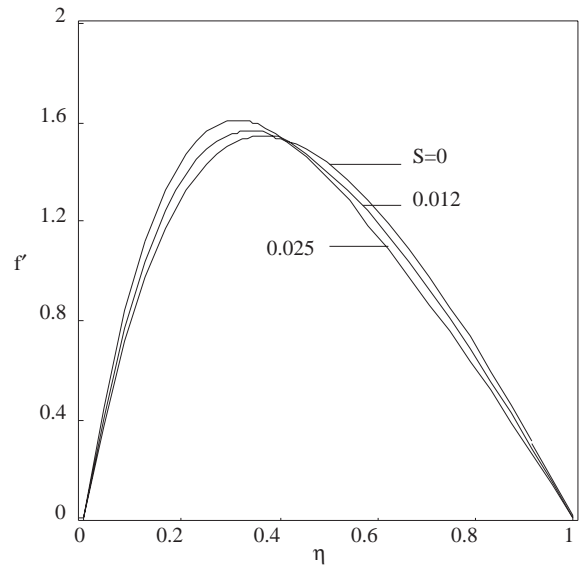
Figure 4. Tangential velocity profiles for Re = 10

Figures 2 and 3 depict the normal velocity component for various values of the elastic number keeping Re fixed at 10 and 20, respectively. It is clear from these figures that the elastic elements of the fluid increase the normal velocity at any point. The tangential velocity profiles are presented in Figures 4 and 5 for the same values of cross-flow Reynolds number and the elastic number. It is interesting to

Table 1. Missing initial conditions

Re	$f_0''(0)$	$f_0'''(0)$	$f_1''(0)$	$f_1'''(0)$	$h_0'(0)$	$h_1'(0)$
1	6.454264	-14.365855	0.519324	- 2.540334	0.490902	0.565135
10	10.036772	-38.102419	78.281028	-525.642416	0.393128	4.747072
20	13.003869	-65.348653	273.285181	-2360.004261	0.326508	6.576279
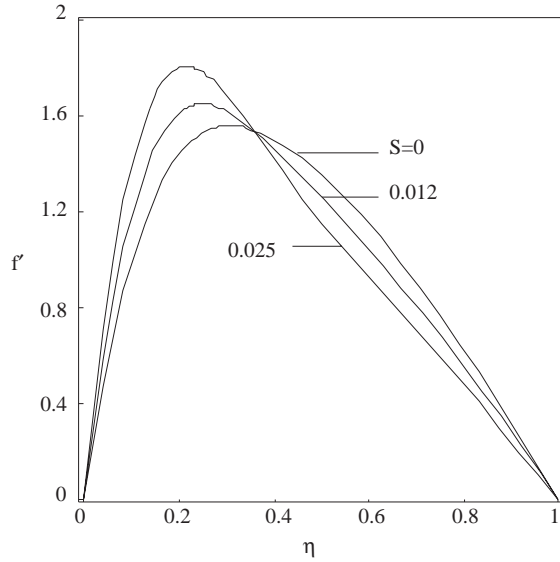
Figure 5. Tangential velocity profiles for Re = 20
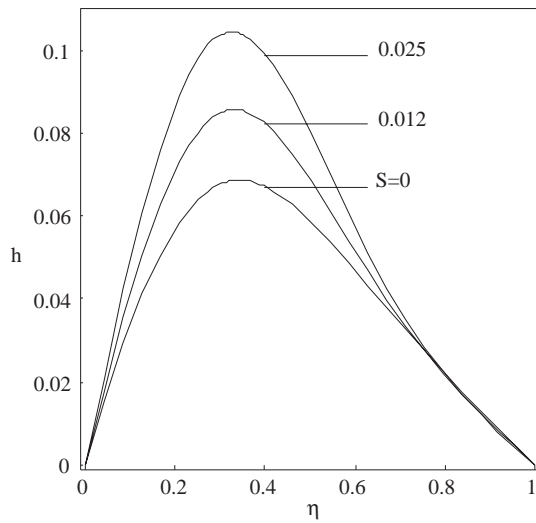
Figure 6. Axial velocity profiles for Re = 10

ber, the point at which maximum velocity occurs moves away from the porous plate. Moreover, the elastic elements of the fluid make this point closer to the impermeable wall. On comparing Figure 2 with Figure 3, or Figure 4 with Figure 5, we arrive at the conclusion that the flow behaviour remains the same, but the difference in magnitudes of Newtonian and viscoelastic velocity profiles goes on increasing.
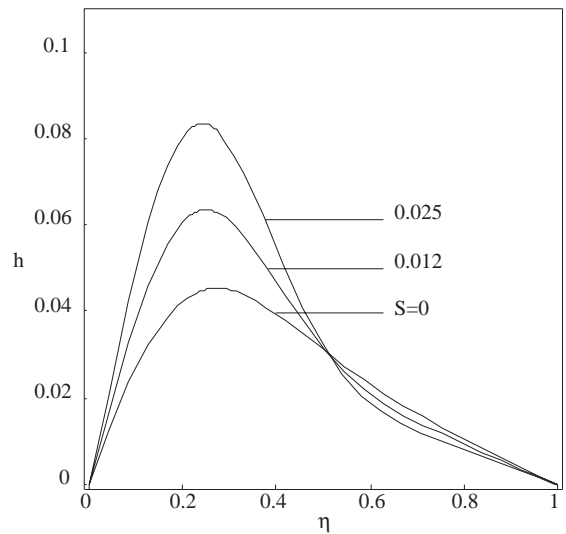
Figure 7. Axial velocity profiles for Re = 20

The axial component of velocity is due to the action of gravity along the z-axis. This velocity component is shown in Figures 6 and 7. It is obvious from these figures that the velocity profiles decrease with the increase in the cross-flow Reynolds number. On the other hand, the elasticity of the fluid, i.e. S, affects the axial velocity profiles in different ways, depending on the chosen values of the cross-flow Reynolds number. For instance, when Re = 10, we notice that the axial velocity for a viscoelastic fluid is more than that for a Newtonian fluid. However, when Re = 20, the curves of the axial component of velocity for different values of elastic number intersect at a common point, say at about $\eta = 0.5$. Up to this point, elastic elements of the fluid increase

note that the tangential velocity increases with an increase in the elastic number S, up to approximately $\eta = 0.4$, and thereafter decreases with increasing S. Again from these figures we observe that with an increase in the value of the cross-flow Reynolds num-

the axial velocity. But an opposite effect is observed beyond this point, that is, the axial velocity slightly decreases with an increase in the elasticity of the fluid.
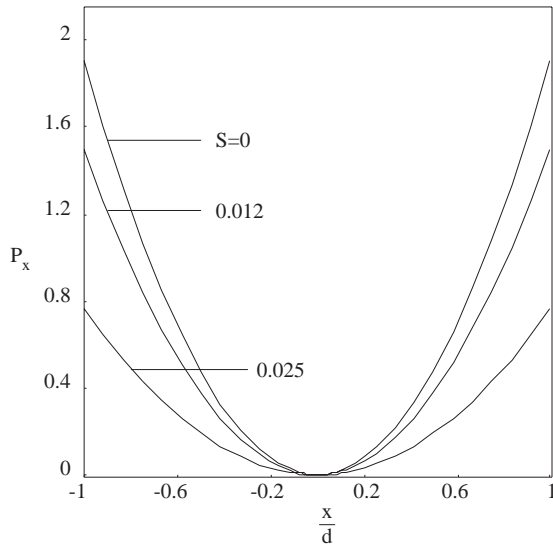
Figure 8. Pressure variation in the x direction for Re = 10

Figures 8 and 9 represent the pressure variations in the x and y directions, respectively. An examination of these figures shows that the elasticity of the fluid decreases the pressure variations in both directions. In Table 2, the shear stresses on the walls of the channel are listed for various combinations of cross-flow Reynolds number and elastic number. We observe from this table that the main effect of elastic number on the shear stresses in the x and z directions on the impermeable wall is to increase their values, whereas it is to decrease those on the porous plate. Furthermore, it is evident that as the cross-

flow Reynolds number increases, the change in shear stresses on the walls is much more noticeable.
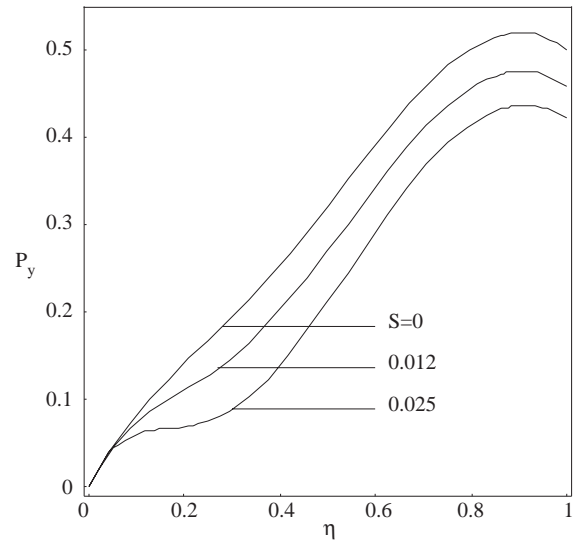
Figure 9. Pressure variation in the y direction for Re = 10

In order to investigate the effect of the elasticity of the fluid on the heat transfer on walls, we have presented the values of $\theta'(0)$ and $\theta'(1)$ in Table 3 for different values of cross-flow Reynolds number, Peclet number, and elastic number. For high Peclet numbers, the heat transfer on the impermeable plate at $\eta = 0$ is considerably higher than that on the porous plate at $\eta = 1$ in both cases, i.e. Newtonian and non-Newtonian fluid. Again from Table 3, we notice that with an increase in the elastic number, the heat transfer increases for the impermeable plate, whereas it decreases for the porous plate. This change in heat transfer on the walls is more pronounced for the case of large cross-flow Reynolds number and Peclet number.

Table 2. Shear stresses on walls

Re	$\tau_{xy}(0)$	$\tau_{zy}(0)$	$\tau_{xy}(1)$	$\tau_{zy}(1)$	S
10	10.036772	0.393128	-3.684423	-0.103703	0
	10.976144	0.450093	-3.567867	-0.089773	0.012
	11.993797	0.511805	-3.397018	-0.068475	0.025
20	13.003869	0.326508	-3.241770	-0.050438	0
	16.283291	0.405424	-2.989399	-0.045924	0.012
	19.835998	0.490915	-2.683713	-0.045746	0.025

Table 3. Heat transfer on walls

	Pe = 1		Pe = 8		Pe = 15		
Re	$\theta'(0)$	$\theta'(1)$	$\theta'(0)$	$\theta'(1)$	$\theta'(0)$	$\theta'(1)$	S
1	1.153104	0.693849	2.025087	0.034803	2.571836	0.001262	0
	1.153159	0.693810	2.025475	0.034781	2.572416	0.001261	0.012
	1.153219	0.693768	2.025895	0.034756	2.573044	0.001259	0.025
10	1.177354	0.677910	2.198961	0.026567	2.834805	0.000719	0
	1.183094	0.674514	2.240930	0.025015	2.898132	0.000633	0.012
	1.189325	0.670843	2.286138	0.023424	2.965693	0.000552	0.025
20	1.189583	0.671447	2.294248	0.023636	2.984769	0.000561	0
	1.203184	0.664659	2.400935	0.020822	3.150682	0.000429	0.012
	1.218006	0.657335	2.515618	0.018103	3.325191	0.000319	0.025

Conclusions

The present paper is concerned with the steady three-dimensional flow of a Walter's B′ fluid between two parallel vertical walls. By means of similarity transformations, the governing equations are reduced to set of ordinary differential equations. Numerical calculations have been carried out for various values given to the non-dimensional parameters Re, S and Pe and qualitatively significant contribution of the elastic parameter S to the velocity components, pressure variations in the x and y directions, shear stresses and heat transfer on the walls of the channel have been pointed out. From the present investigations, we may conclude the following:

1. Elasticity of the fluid increases the normal velocity at any point and the cross-flow Reynolds number increases it further.

2. Tangential velocity increases with an increase in the elastic number S, up to approximately $\eta = 0.4$, and thereafter decreases with increasing S.

3. Elastic elements in the viscous fluid affect the axial velocity component in different ways, depending on the values given to the cross-flow Reynolds number.

4. Pressure variations in the x and y directions decrease with an increase in the value of elastic number.

5. For a Newtonian fluid, the shear stresses on the impermeable wall are less than corresponding shear stresses for a viscoelastic fluid. The reverse is true for the porous wall.

6. Presence of viscoelasticity leads to an increase in heat tranfer on the impermeable wall, but a decrease in heat transfer on the porous wall.

7. For a high Peclet number, heat tranfer on the impermeable wall is considerably higher than that on the porous wall.

8. The above-mentioned changes in tangential velocity, shear stresses and heat transfer are much more noticable for the case of a large cross-flow Reynolds number.

Acknowledgements

Nomenclature

c_p	specific heat at constant pressure, $L^2T^{-2}\vartheta^{-1}$
e	rate of strain tensor, T^{-1}
g	gravitational acceleration vector, LT^{-2}
I	identity tensor, dimensionless
k	thermal conductivity, $MLT^{-3}\vartheta^{-1}$
k_0	short memory coefficient, ML^{-1}
L, B, d	dimensions of the channel, L
Pe	Peclet number, dimensionless
p	pressure, $ML^{-1}T^{-2}$
P_x, P_y	pressure variations in the x and y directions, dimensionless
Re	cross-flow Reynolds number, dimensionless
S	elastic number, dimensionless

T	temperature, ϑ	**v**	velocity vector, LT^{-1}
T	Cauchy stress tensor, $ML^{-1}T^{-2}$	η_0	limiting viscosity at small rate of shear, $ML^{-1}T^{-1}$
T_0, T_1	temperatures of the walls, ϑ		
t	time, T	ρ	density, ML^{-3}
U	uniform injection velocity, LT^{-1}	τ	relaxation time, T
u, v, w	components of the velocity vector, LT^{-1}	τ_{xy}, τ_{zy}	shear stresses on walls, dimensionless

References

Ascher, U., "Solving Boundary Value Problems with a Spline-Collocation Code", J. Comp. Phys., 34, 401-413, 1980.

Barış, S., "Injection of a Non-Newtonian Fluid through One Side of a Long Vertical Channel", Acta Mech., 151, 163-170, 2001.

Beard, D.W. and Walters. K., "Elastico-Viscous Boundary Layer Flows. Part I. Two-Dimensional Flow near a Stagnation Point", Proc. Camb. Phil. Soc., 60, 667-674, 1964.

Berman, A.S., "Laminar Flow in Channels with Porous Walls", J. Appl. Phys., 24, 1232-1235, 1953.

Choi, J.J., Rusak, Z. and Tichy, J.A., "Maxwell Fluid Suction Flow in a Channel", J. Non-Newtonian Fluid Mech., 85, 165-187, 1999.

Cox, S.M., "Two Dimensional Flow of a Viscous Fluid in a Channel with Porous Walls", J. Fluid Mech., 227, 1-33, 1991.

Huang, C.L., "Application of Quasilinearization Technique to the Vertical Channel Flow and Heat Convection", Int. J. Non-Linear Mech., 13, 55-60, 1978.

Schlichting, H., "Boundary-Layer Theory", McGraw-Hill, 40-41, 362-364, 1968.

Sharma, P.R. and Chaudhary, R.C., "Fluid Injection of a Rivlin-Ericksen Fluid through One Side of a Long Vertical Channel", Bull. Tech. Univ. Istanbul, 35, 175-185, 1982.

Singh, K.D., "Three Dimensional Couette Flow with Transpiration Cooling ", Z. angew. Math. Phys., 50, 661-668, 1999.

Skalak, F.M. and Wang, C.Y., "On the Nonunique Solutions of Laminar Flow through a Porous Tube or Channel", SIAM J. Appl. Math., 34, 535-544, 1978.

Terrill, R.M. and Shrestha, G.M., "Laminar Flow through Parallel and Uniformly Porous Walls of Different Permeability", Z. angew. Math. Phys., 16, 470-482, 1965.

Wang, C.Y. and Skalak, F., "Fluid Injection through One Side of a Long Vertical Channel", AIChE J., 20, 603-605, 1974.